Heliyon 10 (2024) e38793

Contents lists available at ScienceDirect

Heliyon

journal homepage: www.cell.com/heliyon

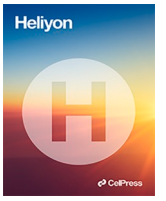

Research article

Revolutionizing fast disintegrating tablets: Harnessing a dual approach with porous starch and sublimation technique

Sameer J. Nadaf [a,*], Pranav L. Savekar [b], Durgacharan A. Bhagwat [c], Komal V. Dagade [d], Shailendra S. Gurav [e]

[a] *Bharati Vidyapeeth College of Pharmacy, Palus 416310, Maharashtra, India*
[b] *Shivraj College of Pharmacy, Gadhinglaj 416502, Maharashtra, India*
[c] *Bharati Vidyapeeth College of Pharmacy, Kolhapur 416013, Maharashtra, India*
[d] *Medical Center, Tasgaon 416312, Maharashtra, India*
[e] *Department of Pharmacognosy, Goa College of Pharmacy, Goa University, Goa 403001, India*

A R T I C L E I N F O

Keywords:
Mung bean
Vigna radiata
Superdisintegrant
Camphor
Oral drug delivery

A B S T R A C T

This study investigates the transformation of neat starch (NS) from mung beans into porous starch (PS) for the formulation of fast-disintegrating tablets (FDTs) using the sublimation technique, contrasting their performance with superdisintegrants such as sodium starch glycolate (SSG) and croscarmellose sodium (CS). Camphor was used as a sublimating agent. The interaction between drug and excipients was analyzed using Fourier-transform infrared spectroscopy (FTIR), while preformulation assessments were conducted on powder blends. Model drug Diclofenac sodium (DL)-loaded FDTs were prepared via direct compression technique. Thermal behavior and crystalline properties were evaluated using differential scanning calorimetry (DSC) and powder X-ray diffraction (PXRD), respectively. Compressibility of tablets was assessed through Heckel and Kawakita analyses. Post-compression evaluations encompassed hardness, thickness, *in vitro* disintegration, and dissolution studies. FTIR analysis indicated the absence of chemical interactions among constituents, while precompression analyses confirmed favorable flow properties of the blends. Heckel analysis supported the material's notable compressibility. Microscopic examination revealed the formation of pores on the tablet surface due to the sublimation process. Integration of PS significantly accelerated the disintegration time of FDTs, with durations ranging from 50 to 82 s, compared to 76–104 s for NS-FDTs. While PS-FDTs exhibited a longer disintegration time compared to SSG, they demonstrated faster disintegration compared to croscarmellose sodium. A significant disparity ($p<0.01$) in drug release at 60 min was observed between SSG and PS-FDTs, with DP3 achieving 97.65 % drug release. Most batches followed the Korsmeyer-Peppas model, except for DN2 and DN3, which adhered to Higuchi-matrix drug release kinetics. Stability assessments after 90 days revealed no significant differences ($p>0.05$). Conclusively, this study highlights the effectiveness of PS and the sublimation method in creating FDTs with enhanced drug release properties.

* Corresponding author.
E-mail address: sam.nadaf@rediffmail.com (S.J. Nadaf).

https://doi.org/10.1016/j.heliyon.2024.e38793
Received 26 February 2024; Received in revised form 28 September 2024; Accepted 30 September 2024
Available online 2 October 2024

1. Introduction

Oral drug delivery stands as a cornerstone in pharmaceutical practice, cherished for its simplicity of application and patient adherence. Despite notable strides in drug delivery modalities, oral administration remains the preferred conduit for active pharmaceutical ingredients [1]. Nevertheless, traditional dosage forms like tablets and capsules pose hurdles such as swallowing difficulties and the ingestion of unpalatable medications, disproportionately impacting demographics such as pediatric and geriatric patients, as well as individuals with restricted access to water [2]. In response to these challenges and with the aim of augmenting patient compliance, innovative formulations such as fast-disintegrating tablets (FDTs) have emerged. FDTs, also referred to as orally dispersible tablets (ODTs) or rapid dissolve tablets, swiftly disintegrate in the oral cavity without necessitating mastication, typically within a minute [3]. This rapid disintegration, occurring within a mere 5–30 s, is facilitated by the infiltration of saliva into the tablet's microstructure upon placement in the mouth, offering a promising avenue for enhancing drug delivery and patient adherence, especially among vulnerable populations [4].

The formulation of FDTs encompasses a spectrum of excipients, including bulking agents, emulsifiers, organoleptic modifiers, lubricants, and glidants, each serving precise functions within the tablet matrix. Notably, it is the inclusion of superdisintegrants that assumes paramount importance in accelerating tablet disintegration. By catalyzing rapid breakdown upon contact with saliva, superdisintegrants expedite dissolution and subsequent absorption of active pharmaceutical ingredients, thereby amplifying the overall efficacy and patient experience of FDTs [5].

Across the annals of pharmaceutical research, various fast-disintegrating agents have been meticulously studied for their mechanisms governing tablet disintegration, spanning cellulose derivatives, starch derivatives, and synthetic compounds. Among commercially available synthetic superdisintegrants, distinguished examples include croscarmellose sodium (CCS), sodium starch glycolate (SSG), crosspovidone, modified cellulose, and Low-substituted Hydroxypropyl Cellulose (L-HPC) [6]. Additionally, novel formulations such as coprocessed superdisintegrants—Ludiflash, Pharmaburst, modified mannitol, Polacrilin potassium, and Glucidex IT—have emerged, boasting enhanced disintegration properties tailored for fast-disintegrating tablets [7].

Recent inquiries have underscored the promise of exploring superdisintegrants sourced from natural origins. Investigations into materials like guar gum, locust bean gum, and *Plantago ovata* husk have underscored their effectiveness and versatility as credible alternatives to synthetic counterparts in fast-dissolving tablet formulations [8–10]. Leveraging the rapid swelling and disintegration attributes of these natural substances, researchers have demonstrated their utility in augmenting the dissolution and bioavailability of active pharmaceutical ingredients [11]. Such revelations not only underscore the imperative of sustainable and eco-conscious practices in pharmaceutical innovation but also chart a course for novel formulations harnessing the therapeutic bounty of natural reservoirs [12].

Mung bean, scientifically denoted as *Vigna radiata*, a leguminous plant species esteemed for its edible seeds and sprouts, indigenous to the Indian subcontinent [13,14]. Porous starch (PS) derived from mung beans presents a gamut of advantages, including elevated porosity, heightened water absorption capacity, inherent biocompatibility, amplified drug release kinetics, and cost efficiency. Its expansive surface area owing to a porous framework enhances water absorption, precipitating rapid swelling and subsequent tablet disintegration, thereby expediting drug release and absorption. Mung bean PS, being a natural and biocompatible substance, finds favor in pharmaceutical applications, being generally regarded as safe and well-tolerated by the human body. By expediting tablet disintegration and dissolution, PS superdisintegrants bolster the bioavailability and efficacy of drugs, particularly those afflicted with poor solubility or sluggish dissolution rates. Moreover, this starch proffers a cost-effective alternative to conventional synthetic superdisintegrants, potentially curtailing production expenses and lessening reliance on synthetic substrates.

Conventional FDTs face stability, manufacturing, drug loading, and disintegration challenges. They're delicate, affecting dosing accuracy, and require innovative formulations for improved quality and performance [4]. Porous tablets represent a cutting-edge solid dosage form distinguished by their low density and intricate pore structures, facilitating substantial surface area for enhanced drug delivery [15,16]. This method holds promise for boosting tablet dissolution rates through heightened hydrophilicity, enhanced swelling capabilities (wettability), and accelerated disintegration [17]. Porous tablets can be crafted through a variety of advanced techniques, including sintering, gel casting, freeze drying, sublimation, and emulsion solvent evaporation [18]. The sublimation technique, widely adopted in the industry, enhances dissolution and enables the formulation of fast disintegrating tablets with high porosity [19]. Additionally, the sublimation technique is being considered due to its simplicity, ease of implementation, and cost-effectiveness [20]. Moreover, prior researchers have leveraged this technique to augment the solubility of BCS class II drugs, namely, atorvastatin trihydrate calcium [18], meclizine hydrochloride [19], ondansetron [21], lovastatin [22], lacidipine [23], clonazepam [24], naproxen sodium [25] meloxicam [26], and flurbiprofen [27].

Thus, the crux of the present study lies in harnessing mung bean PS as a novel disintegrating agent in model drug diclofenac sodium-based fast disintegrating tablet formulations (DL-FDTs). By leveraging the unique properties of mung bean PS, we aim to enhance understanding of drug dissolution kinetics through the application of the sublimation method. This pioneering study integrates two innovative approaches i.e. the utilization of mung bean PS and the application of the sublimation technique. Through this dual approach, we seek to elucidate intricate mechanisms governing drug release from tablets, thereby contributing to the development of more effective and efficient pharmaceutical formulations.

2. Material and methods

2.1. Materials

Diclofenac sodium (DL), microcrystalline cellulose, sodium starch glycolate, camphor, croscarmellose cellulose, n-hexane, sodium hydroxide, lactose and magnesium stearate were procured from Research-Lab Fine Chem Industries Ltd., Mumbai, India. Double distilled water was used for the experiments.

2.2. Collection and authentication

In August, a *Vigna radiata* plant was gathered from the Khanapur district in India. Dr. S. M. Shendage of the Department of Botany at Balwant College, Vita, India, further taxonomically identified the sample after it had been air-dried and sealed in airtight bags. Following that, a voucher herbarium specimen sheet was deposited to Department of Pharmacognosy, Bharati Vidyapeeth College of Pharmacy, Kolhapur (Voucher No. BVCPK/Pcong/19–20/08).

2.3. Isolation and preparation of starch

2.3.1. Isolation of starch

Starch from mung bean was isolated using wet milling scheme previously reported by Abdel-Rahman et al. [28], and Singh et al. [29], with little modifications. Properly washed mung bean seeds (500 g) were steeped in water (1 L) and kept overnight at room temperature. The steeping solution was discarded and seeds were washed 2–3 times with distilled water. Washed seeds were ground in a blender for 4–5 min at a fixed ratio of bean: water (1:3) followed by filtration through a fine cloth. Grinding and filtration are repeated on residual material. The obtained filtrate was allowed to settle for 0.5 h and then centrifuged at 5000 rpm for 8 min followed by protein-rich layer separation. After adding 5 mL of water to the solid starch mass and centrifuging it, pure starch was separated. Native starch (NS) was dried at 45 °C for 24 h, ground, sieved and stored properly until further use.

2.3.2. Preparation of PS

At room temperature, 40 mL of distilled water were well mixed with 10 g of NS. Next, while swirling quickly, starch dispersion was added to the boiling water. A translucent gel was generated by gradually lowering the temperature to room temperature and continuing to stir. To reach an equilibrium state, the gel was kept overnight in excess water at 8 °C. After that, ethanol was used to exchange solvents with the gel. To preserve its porous structure, the gel was allowed to acclimate and was then kept in ethanol at 8 °C for 48 h. Once the gel reached its equilibrium state, it was dried in an oven set at 30 °C [30–32].

2.4. Characterization of NS and PS

2.4.1. Determination of chemical composition and micromeritic properties

Using previously published techniques, starch was assessed for several parameters, including melting point, initial chemical test for biological components, moisture %, protein, ash percentage, pH, swelling power and solubility [33–39]. Micromeritic properties of NS and PS were estimated using earlier reported protocols [38–40]. Detailed procedures are shown in supplementary material.

2.4.2. Spectroscopic and thermal analysis

Fourier Transform Infrared (FTIR) spectrum of starches was recorded using Infra-red spectrophotometer (Jasco-V-530 model). About 2 mg of sample is ground thoroughly with KBr; uniformly mixed sample kept in sample holder and spectrum was recorded over the wave number 400-4000 cm^{-1}. The crystalline properties of NS and PS were studied using Powder X-Ray Diffraction (PXRD) study. Samples were irradiated with monochromatized Cu Kα radiation (1.742 Å) and analyzed over a diffraction angle (2θ) between 5° and

Table 1
Composition of prepared DL-FDTs.

Composition (mg)	Function	DN1	DN2	DN3	DP1	DP2	DP3	DS1	DS2	DS3	DC1	DC2	DC3
DL	Drug	50	50	50	50	50	50	50	50	50	50	50	50
NS	Disintegrant	4	8	12	–	–	–	–	–	–	–	–	–
PS	Disintegrant	–	–	–	4	8	12	-	–	–			
SSG	Superdisintegrant	–	–	–	–	–	–	4	8	12	–	–	–
Croscarmellose sodium	Superdisintegrant	–	–	–	–	–	–	–	–	–	4	8	12
Sodium saccharine	Taste masking agent	10	10	10	10	10	10	10	10	10	10	10	10
Microcrystalline cellulose	Dry binding Agent	90	90	90	90	90	90	90	90	90	90	90	90
Camphor	Subliming agent	50	50	50	50	50	50	50	50	50	50	50	50
Talc	Lubricant	3	3	3	3	3	3	3	3	3	3	3	3
Magnesium stearate	Lubricant	3	3	3	3	3	3	3	3	3	3	3	3
Lactose	Filler	80	76	72	80	76	72	80	76	72	80	76	72
Total weight	–	290	290	290	290	290	290	290	290	290	290	290	290

All ingredients are in mg.

50° on Rigaku Miniflex- 600 X-ray Diffractometer. The voltage and current used were 30 kV. Thermal behavior of NS and PS was analyzed by differential scanning calorimeter (TA instruments, model SDT 2960, USA) equipped with intercooler and refrigerated cooling system.

2.4.3. Scanning electron microscopy (SEM)

The habitat of the NS and PS was examined using a scanning electron microscope (TESCAN VEGA3). The samples were affixed onto the SEM stage, coated with a thin layer of gold using an ion sputter, and observed under an operating voltage of 10 kV.

2.5. Formulation of compacts using Vigna radiata starch

2.5.1. Formulation of fast disintegrating tablets (FDTs)

FDTs containing 50 mg of DL were prepared using the direct compression method. Table 1 presents the formulations used in the study. The disintegration efficiency of PS was compared to two widely used synthetic superdisintegrants: croscarmellose sodium and Sodium starch glycolate (SSG). Different disintegrants, including NS (DN1 - DN3), PS (DP1 - DP3), SSG (DS1 - DS3), and Croscarmellose sodium (DC1 - DC3), were incorporated in varying amounts into a fixed quantity of drug and other excipients to produce a total of 12 batches. To ensure uniformity, each ingredient was individually passed through a #60 sieve before thorough mixing. The combined material was then directly compressed into tablets using a 16-station rotary tablet punching machine. Subsequently, the compressed tablets underwent a sublimation process in a vacuum oven for 6 h at 50 °C. This sublimation process involved several steps. First, the compressed tablets were carefully arranged on trays and placed inside a vacuum oven. Once the oven was sealed, a vacuum was applied to create a low-pressure environment. The oven temperature was maintained at a steady 50 °C throughout the process, ensuring that the volatile components within the tablets were gently heated. Under the combined effect of low pressure and controlled heating, the volatile components within the tablets underwent sublimation, transitioning directly from a solid state to a gaseous state without passing through a liquid phase. As the volatile components vaporized, they were removed from the oven by the vacuum system, which was crucial for achieving the desired porosity in the tablets. After 6 h, the heating was stopped, and the tablets were allowed to cool gradually while still under vacuum, preventing any condensation of the removed volatiles back into the tablets. This step enhanced the porosity of the tablets, improving their disintegration time and overall dissolution profile, and making the tablets more effective for rapid drug release [41].

2.6. Evaluation of compacts

2.6.1. Precompression evaluation

2.6.1.1. Micromeritic properties. Bulk density, tapped density, angle of repose, Carr's compressibility index and Hausner's Ratio was determined (refer to additional information).

2.6.1.2. Compression study

2.6.1.2.1. Heckel study. Herein, matrices underwent compaction using a hydraulic press featuring a 10 mm flat-faced punch, applying varying pressures from 1 to 3.5 tons for a duration of 1 min each (n = 3 replicates). Following a 24 h relaxation period, measurements were taken for thickness (t), diameter (D), weight of compacts (W), and the force (F) necessary for compact fracture. Tensile strength (σt) was determined using the formula $\sigma t = 2F/(\pi Dt)$. Furthermore, the dataset underwent analysis utilizing the Heckel Eq. (1), a sophisticated method to assess powder compaction behavior and characterize material properties under pressure.

$$\ln\left(\frac{1}{1-p_r}\right) = KyP + A \quad (1)$$

In the Heckel Equation, where ρr represents the packing fraction of the tablet, the slope K denotes the Heckel constant, calculated as K = 1/MyP where MyP is the mean yield pressure. Additionally, the intercept 'A' indicates densification at low pressure [42].

2.6.1.2.2. Kawakita analysis. The degree of volume reduction (C) to gauge compression was determined through the Kawakita analysis. The experimental process involved recording the reduction in volume (n/c) corresponding to the number of tappings (n), employing a bulk density apparatus. A comprehensive plot of n/c against n was meticulously constructed. The intricate estimation of parameters, including C, constant 'a', and 'b', was carried out using below equations (2) and (3),

$$\left(\frac{n}{C}\right) = \left(\frac{n}{a}\right) + \left(\frac{1}{Ab}\right) \quad (2)$$

$$C = \left(\frac{V_0 - V_\infty}{V_0}\right) \quad (3)$$

Where, 'a' represents compactibility, while 'b' stands for plasticity, reflecting its deformation under pressure. V_0 denotes the initial bulk volume, and V_∞ represents the volume after tapping [42].

2.6.2. Post compression evaluation

All the tablets were evaluated for different physical parameters as weight variation, hardness, friability, drug content and *in vitro* dissolution study as per reported methods [41,43–45]. Parameters were estimated before and after sublimation process. Detailed protocols are mentioned in supplementary file.

2.6.2.1. Wetting time and water absorption ratio. A double folded tissue paper was placed in Petri dish. 6 mL of water containing a soluble dye (eosin) was added to Petri dish. A tablet (pre-weight) was carefully placed on surface of tissue paper. The time required for water to reach the upper surface of the tablet was noted as the wetting time. The wetted tablet was then weighed and the water absorption ratio (R) was determined by using eq. (4) [41,43].

$$R = \frac{100 \times (W_b - W_a)}{W_b} \times 100 \quad (4)$$

Where, W_a and W_b are the weights of tablet before dry weights and after water absorption (wet weight) respectively.

2.6.2.2. Weight loss by sublimation. The weight of twenty tablets from each batch was measured both before and after the sublimation process. The weight loss resulting from sublimation was determined using the provided eq. (5):

$$\text{Weight loss} = \frac{(W_I - W_F)}{W_I} \times 100 \quad (5)$$

Where, W_I and W_F are weight before and after sublimation, respectively.

2.6.2.3. Estimation of tablet porosity. The porosity of the tablets was calculated using the weight of the tablet (W), the tablet volume (V), and the true density of the powder (ρ) according to eq. (6) [46]:

$$\%\ porosity = \left[1 - weight\ of\ tablet \frac{(W)}{Volume}(V) \times Density\ (\rho)\right] \quad (6)$$

2.6.2.4. Surface morphology. Surface morphology of market formulation and tablets of optimized batch before and after sublimation was assessed using Motic microscope.

2.6.2.5. Spectroscopic and thermal behavior. FTIR spectra of NS, PS, DL, physical mixture (PM) and optimized formulation was determined using FTIR spectrophotometer. Crystallinity of prepared mass was checked by PXRD study. Thermal behavior of PS, DL and optimized batch (DP3) was analyzed by Differential Scanning Calorimeter (DSC) (TA instruments, model SDT 2960, USA) equipped with intercooler and refrigerated cooling.

2.6.2.6. In vitro disintegration test. Disintegration of the mini-tablets was performed according to earlier method with some modifications [47]. Ten randomly selected tablets were placed individually in a Petri dish containing 20 mL of 0.05 M phosphate saline buffer (pH 6.8, 37 °C) and the time required for the tablet to completely disintegrate into fine particles was meticulously recorded for accuracy. According to the European Pharmacopoeia (Ph. Eur.), orally disintegrating tablets should disintegrate within 3 min. Measurements were carried out in replicates of three tablets (n = 3).

2.6.2.7. In vitro dissolution studies. With slight modification in earlier reports [41,48–51], dissolution rate was studied using USP type II paddle dissolution apparatus, in 900 mL of phosphate buffer pH 6.8 at 37 ± 0.5 °C at 100 rpm/min. Aliquot (5 mL) of dissolution medium was withdrawn at regular time interval and the same volume of pre-warmed (37 ± 0.5 °C) fresh dissolution medium was added. The samples were filtered and DS content in each sample was analyzed after suitable dilution by Shimadzu UV-spectrophotometer at 276 nm [41]. The quantity of DL was quantified utilizing equation Y = 4.91X - 0.734 (R^2 = 0.9945), which was derived from the calibration plot of DL in buffer pH 6.8. Subsequently, the % drug release data was subjected to fitting with various drug release kinetic models, encompassing zero-order ($Q = Q_0 + k_0t$), first-order ($\ln Q = \ln Q_0 + k_1t$), Higuchi matrix ($Q = k_Ht^{1/2}$), Hixson-Crowell ($Q_0^{1/3} - Q_R^{1/3} = K_s\,t$), and Korsmeyer-Peppas ($Q/Q_T = k_{kp}t^n$) models, aiming to ascertain the optimal fitting model. Furthermore, an inter-batch comparison was conducted based on mean dissolution time (MDT) and dissolution efficiency (DE). DE was computed at various time intervals (3, 5, 10, 15, 20, 30, 45, and 60 min) employing eq. (7):

$$DE = \frac{\int_{t_1}^{t_2} y.dt}{y_{100\times(t_2-t_1)}} \times 100 \quad (7)$$

Where, y is drug dissolved (%), DE is the area under the dissolution curve (AUC) between t_1 and t_2 and represented as a percentage of AUC of trapezoid corresponding to 100 % dissolution within the same time.

2.6.2.8. Stability studies. In this investigation, the refined formulations underwent storage under controlled conditions at 25 °C ± 2 °C/60 % RH ± 5 % RH within hermetically sealed containers for a duration of 90 days, with the aim of examining the preliminary stability of the compressed porous tablets. Evaluations encompassing hardness, friability, disintegration time, drug content, and dissolution rate were conducted on stored samples at both the 30th and 90th day marks. Subsequently, the acquired data from these time points were juxtaposed with the initial day results to discern any alterations over the storage period.

3. Results and discussion

3.1. Chemical composition

The starch extracted from *Vigna radiata* underwent isolation via water filtration methodology. Analysis revealed that the isolated starch, both native and porous, displayed melting points ranging from 90 to 95 °C and 89–95 °C respectively, aligning with the parameters outlined in Hoover et al.'s data [52]. Initial chemical assays indicated positive outcomes for amylose, carbohydrates, proteins, and lipids, signifying their presence within the isolated native starch. These findings supplement previously reported data encompassing ash content, pH levels, drying kinetics, moisture content, and protein concentration [53].

At the initial stage (time 0), the average moisture content measured 1.43 ± 0.006. By the time 1.75 h had elapsed, this moisture content had decreased substantially to 0.02 ± 0.001, indicating the completion of the drying process for the native starch (NS). Graph (Fig. S1) depicts a rapid decline in moisture content initially, followed by a more gradual reduction as drying time extended from 15 min to 105 min. This drying trend mirrors observations made by the Ajala et al., affirming consistency in the drying kinetics of the native starch sample [54]. The graphical representation (Fig. S2) illustrates a diminishing drying rate as the moisture content decreases. Corresponding data detailing this relationship can be found in Table S1.

Drying was maintained until achieving steady moisture content. Increasing the drying temperature facilitated heat transfer, thereby shortening the overall duration of the drying process. It is evident that prolonging time at higher moisture content significantly impacts drying rates, whereas decreasing temperature becomes essentially insignificant as drying progresses. Moreover, initial drying rates or moisture losses were observed to be faster. As the drying process advances, moisture availability may decrease, potentially leading to a decline in drying rate. Case hardening may also contribute to this decrease. Additionally, the development of shrinkage, resulting in decreased porosity of the sample as drying progresses, could be another factor in the reduction of drying rate. As drying time increased, the moisture ratio decreased exponentially, indicating that internal mass transfer was governed by diffusion, as evidenced by the continuous decline in the moisture ratio.

3.2. Micrometrics properties

The angle of repose is a measure of the internal friction of a material. Lower angles of repose generally indicate better flow properties. The values (Table 2) obtained suggest that both NS and PS exhibit excellent flowability, with PS demonstrating a slightly lower angle of repose compared to NS. This indicates that PS might flow marginally better than NS. Hausner's ratio is the ratio of tapped density to bulk density. Values less than 1.25 generally indicate good flowability. Both NS and PS have Hausner's ratios close to 1.1 (Table 2), signifying that both materials have very good flow characteristics. This further confirms the observations made from the angle of repose measurements. A Carr's index below 15 % typically indicates good flowability. The values for NS and PS are both below 15 % (Table 2), corroborating the excellent flowability of these materials as suggested by the angle of repose and Hausner's ratio. Comparative analysis with maize starch reveals that both NS and PS exhibit superior flowability [40].

The marginal difference between tapped density (0.71 ± 0.01 gm/mL) and bulk density (0.64 ± 0.01 g/mL) for NS suggests minimal inter-particle interactions, further supporting its free-flowing nature. This attribute can be attributed to the uniform particle size distribution, low friction coefficient (ψ), and low moisture content of NS which is considered to be beneficial for the porous tablets as it may help in enhancement of the solubility and dissolution rate by means of increasing the wettability, swelling index and rapid

Table 2
Flow properties of Precompression blend.

Batches/Starch	Bulk density (g/mL)	Tap density (g/mL)	Angle of repose (θ)	Hauser's ratio	Carr's index (%)	Inter particle porosity
NS	0.64 ± 0.01	0.71 ± 0.01	30.92 ± 0.84	1.11 ± 0.02	9.80 ± 1.27	0.29 ± 0.02
PS	0.80 ± 0.01	0.90 ± 0.01	27.31 ± 0.02	1.13 ± 0.01	11.15 ± 1.06	0.13 ± 0.02
DN1	0.82 ± 0.01	0.89 ± 0.00	29.14 ± 0.23	1.09 ± 0.02	8.24 ± 1.30	NA
DN2	0.81 ± 0.01	0.89 ± 0.01	28.81 ± 0.68	1.09 ± 0.01	8.27 ± 0.62	NA
DN3	0.81 ± 0.01	0.89 ± 0.01	27.30 ± 0.78	1.09 ± 0.01	8.27 ± 1.25	NA
DP1	0.83 ± 0.01	0.89 ± 0.01	29.14 ± 1.27	1.07 ± 0.02	6.38 ± 1.69	NA
DP2	0.81 ± 0.01	0.89 ± 0.00	28.75 ± 1.04	1.09 ± 0.01	8.61 ± 0.65	NA
DP3	0.83 ± 0.02	0.88 ± 0.01	28.03 ± 1.74	1.07 ± 0.02	6.41 ± 1.73	NA
DS1	0.81 ± 0.00	0.89 ± 0.01	27.31 ± 0.87	1.10 ± 0.01	9.33 ± 0.58	NA
DS2	0.81 ± 0.01	0.89 ± 0.01	28.04 ± 0.57	1.09 ± 0.01	8.27 ± 0.62	NA
DS3	0.81 ± 0.00	0.88 ± 0.01	27.98 ± 0.99	1.09 ± 0.01	8.30 ± 0.60	NA
DC1	0.82 ± 0.02	0.90 ± 0.02	28.82 ± 1.24	1.10 ± 0.00	8.89 ± 0.17	NA
DC2	0.82 ± 0.01	0.89 ± 0.00	28.76 ± 1.11	1.09 ± 0.02	8.24 ± 1.30	NA
DC3	0.81 ± 0.00	0.89 ± 0.00	29.13 ± 1.42	1.10 ± 0.00	8.99 ± 0.34	NA

disintegration of the tablets. The presence of inter-particle porosity for PS is deemed advantageous for porous tablets, as it can contribute to the improvement of solubility and dissolution rate. This enhancement is facilitated through the augmentation of wettability, swelling index, and prompt disintegration of the tablets [18].

3.3. SEM study

The SEM microphotographs of both NS (Fig. 1A) and porous starch PS (Fig. 1B) revealed granules with an oval to bean-shaped morphology, characterized by smooth surfaces adorned with shallow grooves devoid of cracks. Notably, PS exhibited the presence of porous structures, clearly indicated by arrows in Fig. 1B, further highlighting the distinct porous nature of the starch after the preparation process. The results indicate that the preparation process effectively induced porosity in the starch granules without compromising their external morphology and surface integrity. Generating pores within the starch matrix could be assigned to several facts. Initially, NS was dispersed in water and added to boiling water, allowing for rapid hydration and swelling of starch granules. As the temperature decreased, gelation might have occurred, potentially forming a network structure that could have trapped water molecules and initiated the formation of void spaces within the gel matrix. Overnight equilibration in cool water could have further stabilized and expanded the gel, potentially enhancing the development of porous structures. Subsequent solvent exchange with ethanol might have aimed to preserve these pores by replacing water molecules while potentially maintaining the gel's structural integrity. Acclimating the gel in ethanol could have facilitated reaching an equilibrium state, which would have been crucial for stabilizing the porous structure. Finally, drying the gel could have removed residual ethanol, solidifying the porous starch matrix.

3.4. Evaluation of compact

3.4.1. Precompression evaluation

In the precompression evaluation across various batches, the bulk density, tap density, and angle of repose values consistently demonstrated excellent flow properties, facilitating direct compression. Assessment of the Carr's index confirms the favorable flowability of the blend. Additionally, results from the Hausner ratio indicate satisfactory flow characteristics. These findings collectively fulfill the requirements for direct compression, affirming the suitability of the material for further processing (Table 2). Good flow properties ensure that the powder can be uniformly distributed and compressed into tablets without issues such as uneven filling or

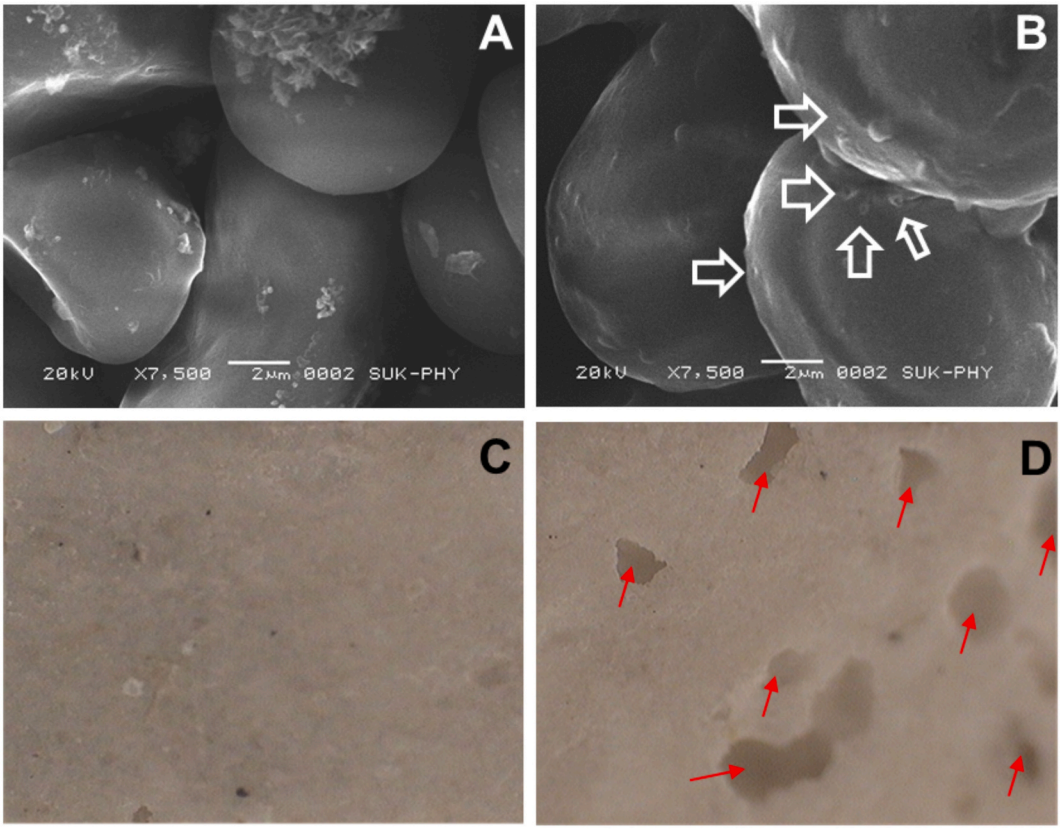

Fig. 1. The SEM photomicrographs of (A) neat starch and (B) porous starch, with the arrow in indicating the presence of the porous structure. Topography images of tablets surface of C) DL-FDT before sublimation and E) DL-FDT after sublimation.

tablet defects. This is crucial for maintaining batch-to-batch consistency and ensuring the quality of the final product.

3.4.2. Compression study

3.4.2.1. Heckel study. The Heckel plot initially displayed a lack of linearity, particularly evident at lower pressures, potentially stemming from intricate particle rearrangements during the nascent stages of compression [42,55]. The notable elevation in the intercept value 'A' signifies a pronounced initial fragmentation, plausibly attributed to the larger particle dimensions of the blended powder and the incorporation of lactose monohydrate, renowned for its propensity for extensive fragmentation [53]. This observation diverges from the findings of Juneja et al., who observed initial linear segments in cornstarch-based conjugates [40]. Subsequent to the phase of initial fragmentation, the compression mixture within the tablet formulation demonstrated plastic deformation concomitant with escalating pressure. Additionally, a decline in porosity at elevated pressures accelerated the densification kinetics. MyP was deduced from the linear segment of the plot.

The Heckel plot (Fig. 2A) and the parameters obtained (Table 3) for DN3, DP3, DC3, and DS3 revealed distinct compaction behaviors and material characteristics: DN3 showed a moderate densification rate, indicating it became denser at a moderate pressure. It started to plastically deform at a higher pressure compared to the other materials and had a relatively lower initial porosity, meaning there was less empty space initially. DP3 demonstrated a higher densification rate, meaning it compacted more readily under pressure. It started to deform plastically at a lower pressure, making it easier to compress. This material had higher initial porosity compared to DN3, indicating that more rearrangement was needed at the beginning. DC3 also showed a good densification rate, indicating good compressibility. It began to deform plastically at a lower pressure than DN3 but slightly higher than DP3 and DS3. Its initial porosity was similar to DP3, suggesting a significant amount of empty space initially. DS3 exhibited the highest densification rate, showing the greatest ability to become denser under pressure. It deformed plastically at the lowest pressure, making it the easiest to compress. Its initial porosity was moderate, similar to DN3. Conclusively, DS3 was the most compressible with the best plasticity and lowest yield pressure. DN3 required the highest pressure to begin deformation and had the lowest densification rate. DP3 and DC3 had intermediate characteristics, with DP3 having slightly lower yield pressure but higher initial porosity compared to DC3. All materials generally fit well with the Heckel model, showing different levels of compressibility and initial porosity.

3.4.2.2. Kawakita analysis. The utilization of Kawakita analysis stands as an invaluable asset in unraveling the intricate nuances of

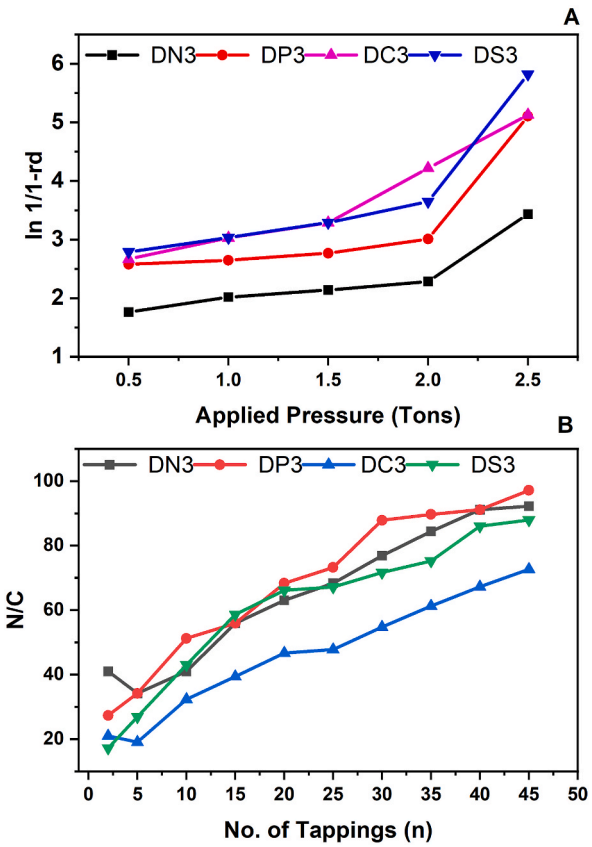

Fig. 2. A) Heckel and B) Kawakita plots.

Table 3
Parameters obtained from Heckel and Kawakita analyses.

Parameters	Kawakita			
	DN3	DP3	DS3	DC3
Slope (m)	1.42	1.63	1.23	1.54
Intercept	32.48	32.34	18.24	25.02
a	0.70	0.61	0.81	0.65
b	0.04	0.05	0.07	0.06
r	0.98	0.95	0.99	0.96
Heckel				
Slope:	0.72	1.08	1.22	1.33
MyP	1.39	0.92	0.82	0.75
Constant	1.25	1.59	1.83	1.71
r	0.88	0.80	0.97	0.87

powder compaction dynamics and prognosticating their densification under applied pressures. Its implementation serves as a cornerstone in refining powder compaction processes, thereby orchestrating the creation of meticulously crafted compacted products endowed with bespoke properties. The comparative analysis of the Kawakita plot parameters reveals distinct characteristics among the powder samples in terms of compressibility, packing density, and the mean yield pressure required to break the particles.

The Kawakita plot (Fig. 2B) parameters for DN3, DP3, DS3, and DC3 revealed distinct compression behaviors. DN3 demonstrated good compressibility and a notable reduction in volume, requiring moderate pressure for effective compaction. It exhibited a balanced performance in terms of packing ability. DP3, while showing the highest rate of compression, achieved the least volume reduction and required slightly more pressure than DN3. This suggests that DP3 compressed readily but with limited volume change. DS3, on the other hand, achieved the greatest volume reduction, indicating it was highly effective at packing. However, it required the most pressure for compression, highlighting its high plasticity. DC3 showed good compressibility and volume reduction, needing a considerable amount of pressure, and demonstrated a balance between plasticity and brittleness. All materials fit well with the Kawakita model, supported by high correlation coefficients, which validated their compression behaviors and packing characteristics.

3.4.3. Post compression evaluation

In the post-compression evaluation, the data presented in Table 4 highlights consistent tablet weights across all formulations, meeting the criteria for acceptable weight variation [24]. Notably, tablet thickness was around 3.65 mm. These findings align closely with a study conducted by Rasoul et al., which investigated Propafenone HCl FDTs containing a subliming agent via direct compression. In their research, tablet hardness ranged from 3.5 to 4.6 kg/cm^2, with a thickness of up to 3.82 mm. The congruence between our results and those reported in the literature further supports the quality and consistency of the formulated tablets [56]. Friability serves as a critical metric for assessing tablet durability, gauging their ability to withstand handling and transit-related stresses. Conventional compressed tablets are generally deemed acceptable if they exhibit a weight loss of less than 1 %. Across all formulations in our study, the percentage friability was comfortably below this threshold. This signifies that the tablets' friability adheres to the prescribed standards, affirming their resilience and appropriateness for pharmaceutical applications. The % porosity of the tablet showed values from 1.36 ± 0.14 % to 23.62 ± 0.14 % for all batches. The water absorption test (%) shows variation in the results where the croscarmellose containing batches showed more percentage (24.29 ± 0.02–26.83 ± 0.02 %) of water absorption compared to that of PS which had lowest value (12.28 ± 0.01–13.22 ± 0.02 %), respectively. The results are similar to that of the Zhang et al., where the porous starch showed low wicking action [57].

The incorporation of PS significantly impacts the disintegration time of tablets. Disintegration time is a critical parameter in the development of FDTs, and it is imperative to optimize this characteristic. In our study, as detailed in Table 4, every batch before sublimation and after sublimation exhibited an approximate disintegration time of less than 150 and 104 s, respectively. The results indicate that variations in starch concentrations influence disintegration, with all batches demonstrating rapid disintegration as the concentration of disintegrants increased in the tablet formulations.

PS notably accelerated disintegration, compared to NS. This trend mirrors findings observed by Odeku et al. [58]. Our study demonstrates superior outcomes compared to the fast-disintegrating tablets (FDTs) formulated by Basu et al. [59], which utilized camphor as a subliming agent. Various batches of tablets containing 10 % camphor, in conjunction with two disintegrants, namely SSG (8–10 %) and Croscarmellose sodium (8 % and 10 %), exhibited prolonged disintegration times relative to our investigation, wherein tablets contained 12.5 % camphor and 3 % PS (DP3). This difference could be attributed to the synergistic effect of porous starch and sublimation. However, our results fall short compared to those reported by Shirsand et al., who developed clonazepam tablets utilizing a sublimation method. This variance could be attributed to the elevated concentrations of Croscarmellose sodium (2–8% w/w) as a superdisintegrant and camphor (20–40 % w/w) employed in their study, exceeding those utilized in ours [24]. These findings underscore the enhanced disintegration performance of our tablet formulations, highlighting the potential of PS in optimizing fast dissolving tablet properties.

The PS-based FDTs exhibited a longer disintegration time compared SSG, but demonstrated faster disintegration in comparison to Croscarmellose. This phenomenon can be attributed to the pores within the PS structure, which absorb water and subsequently swell, leading to rupture of the tablets. The presence of these pores influences various tablet properties, including mechanical strength, tablet

Table 4
Tablet (Post compression) evaluations performed before and after sublimation process.

batches	Before sublimation						After sublimation					
	Weight variation (mg)	Hardness (kg/cm^2)	Thickness (mm)	Friability (%)	Water absorption (%)	Disintegration time (Sec.)	Hardness (kg/cm^2)	Thickness (mm)	Friability (%)	Porosity (%)	Water absorption (%)	Disintegration time (Sec.)
DN1	0.26	3.48 ± 0.34	3.65	0.84 ± 0.15	16.23 ± 1.65	150.30 ± 5.14	3.18 ± 0.26	3.65	0.93 ± 0.18	3.77 ± 0.14	24.29 ± 2.47	104.04 ± 3.57
DN2	0.24	4.15 ± 0.21	3.63	0.86 ± 0.11	13.87 ± 1.32	102.54 ± 6.21	3.88 ± 0.18	3.63	0.85 ± 0.16	1.36 ± 0.14	22.64 ± 1.25	97.67 ± 4.04
DN3	0.28	4.68 ± 0.15	3.64	0.85 ± 0.14	11.65 ± 2.41	92.01 ± 4.32	4.40 ± 0.32	3.64	0.88 ± 0.13	8.68 ± 0.08	22.24 ± 3.07	76.07 ± 3.17
DP1	0.26	3.97 ± 0.47	3.66	0.71 ± 0.13	5.67 ± 0.89	103.74 ± 5.09	3.92 ± 0.49	3.66	0.79 ± 0.11	8.74 ± 0.09	13.21 ± 2.64	82.33 ± 2.60
DP2	1.01	4.08 ± 0.31	3.60	0.71 ± 0.09	8.44 ± 0.93	132.52 ± 4.07	4.06 ± 0.30	3.60	0.85 ± 0.15	23.62 ± 0.14	12.79 ± 2.52	81.19 ± 3.61
DP3	0.15	3.49 ± 0.27	3.63	0.79 ± 0.08	5.08 ± 1.04	96.61 ± 4.38	3.40 ± 0.18	3.63	0.83 ± 0.09	9.89 ± 0.24	12.27 ± 1.99	50.64 ± 3.08
DS1	0.26	3.88 ± 0.15	3.62	0.71 ± 0.09	6.87 ± 1.03	110.43 ± 3.47	3.52 ± 0.22	3.62	0.90 ± 0.10	4.14 ± 0.34	18.56 ± 2.67	80.09 ± 3.86
DS2	0.23	4.57 ± 0.12	3.62	0.68 ± 0.14	11.62 ± 1.54	128.95 ± 5.22	4.37 ± 0.17	3.62	0.76 ± 0.12	8.88 ± 0.41	18.72 ± 2.16	63.53 ± 4.08
DS3	0.17	4.38 ± 0.20	3.64	0.71 ± 0.12	10.25 ± 1.22	97.38 ± 5.61	4.21 ± 0.32	3.64	0.80 ± 0.14	8.58 ± 0.14	19.64 ± 2.46	50.05 ± 2.15
DC1	0.26	4.66 ± 0.17	3.61	0.68 ± 0.11	16.36 ± 1.85	122.16 ± 4.10	4.54 ± 0.34	3.61	0.69 ± 0.16	6.91 ± 0.34	26.82 ± 2.39	80.22 ± 3.77
DC2	0.32	4.13 ± 0.24	3.63	0.68 ± 0.11	16.08 ± 2.19	135.74 ± 5.04	4.10 ± 0.21	3.63	0.72 ± 0.18	11.58 ± 0.22	25.22 ± 3.29	90.04 ± 3.62
DC3	0.26	4.07 ± 0.21	3.62	0.72 ± 0.09	11.37 ± 2.08	110.23 ± 4.62	4.00 ± 0.18	3.62	0.80 ± 0.16	9.99 ± 0.36	24.28 ± 3.10	59.36 ± 3.92

packing fraction, and disintegration. The pores within the tablet structure facilitate the penetration of dissolution media, allowing for efficient interaction with the tablet matrix and contributing to its disintegration. Consequently, while the PS tablet may take longer to disintegrate than SSG, its overall disintegration process is accelerated compared to Croscarmellose due to the unique properties imparted by its porous structure [40,60].

3.4.4. Sublimation of tablets

The tablets' porosity was augmented through the process of sublimation, a phenomenon confirmed by the discernible weight variation observed prior to and post-sublimation. Furthermore, the tablets exhibited commendable mechanical robustness, as indicated by the results of hardness and friability tests (Table 4). Among the formulations examined, DP2 demonstrated the highest percentage of weight loss after sublimation (9.72 %), while DN2 showcased the most minimal deviation (0.41 %), as delineated in Table 5. Notably, the weight loss incurred during the sublimation process remained within acceptable thresholds, with all batches registering a loss of less than 5 %, except for batch DP2. These findings underscore the efficacy of subjecting the tablets to a 6 h drying process, which effectively facilitates the sublimation of the camphor content encapsulated within them.

3.4.5. Surface topography

Fig. 1C and D portray the surface morphology of the newly developed tablets pre-sublimation and after sublimation, respectively. In Fig. 1D, the evolution of pores on the tablet surface is vividly illustrated, a consequence of the sublimation process affecting the sublimating agent. These pores are likely to have expanded into the matrix subsequent to sublimation, resulting in a structure characterized by ample porosity conducive to swift penetration of the dispersion medium. This deduction is substantiated by the enhanced resolution of the tablet's surface images both pre- and post-sublimation. Remarkably, similar observations were documented by Shid et al., thus reinforcing the robustness of our findings [61].

3.4.6. Fourier transform infrared spectroscopy (FTIR)

The interaction study of drug and excipients was studied using FTIR spectroscopy. Fig. 3A displays the FTIR spectrum of *V. radiata* NS, PS, DL, PM and batch DP3. The significant bands at peaks at 3457 cm^{-1} (O–H stretching), 3096 cm^{-1} (C–H stretching), 1044 cm^{-1} (C–N stretching), and 956 cm^{-1} (C–O–H bending) were visible in the FTIR spectrum of NS. The characteristic bands in PS's FTIR spectrum were located at 3596 cm^{-1}, 3019 cm^{-1}, and 1092 cm^{-1}, respectively, and were linked to –OH stretching, C–H stretching, and C–N stretching, respectively. In contrast to the NS spectrum, the PS spectrum displayed peaks that were less intense and smoothed down. This could be the result of pores forming and reducing the starch granule density. The results show that none of the functional groups or characteristics of starch are changed when NS is converted to PS. Since the peaks in this region are vulnerable to structural change, the IR spectra of PS and NS revealed somewhat comparable bands with varying intensities over the range of 1100–900 cm^{-1}, confirming their structural similarity. FTIR spectra of DL shows the peaks at wave numbers 3585 cm^{-1} for O-H, 3385 cm^{-1} for N-H, 1125 cm^{-1} for C-O, C ≡ N, C ≡ C, and 789 cm^{-1} for C-C Stretching.

3.4.7. Powder X-ray diffraction study (PXRD)

PXRD analysis plays a pivotal role in elucidating the crystallinity and structural characteristics of pharmaceutical compounds and their formulations. Fig. 3B displays the PXRD spectrum of *V. radiata* NS, PS, DL, and DP3. In the context of this study, PXRD spectra were employed to discern the crystalline nature of key components, namely NS, PS, DL and optimized batch DP3. The PXRD spectra of NS exhibited a modest 2θ peak at 28°, alongside a limited number of diffraction peaks with low intensity, indicative of its predominantly amorphous nature. Similarly, the PXRD spectra of PS revealed a modest number of diffraction peaks, with a minor peak observed at 28°, also characterized by low intensity, thus suggesting an amorphous character. Amorphous materials tend to dissolve more rapidly compared to crystalline ones due to their higher energy state and greater molecular mobility. Therefore, incorporating amorphous forms of active pharmaceutical ingredients (APIs) or excipients into FDT formulations can potentially enhance dissolution rates and overall bioavailability.

Table 5
Tablet weight (mg) before and after sublimation of camphor add in post compression.

Batches	Sublimation		% weight loss
	Before (mg ± S.D)	After (mg ± S.D)	
DN1	283.28 ± 4.18	278.07 ± 3.15	1.84 ± 0.04
DN2	278.74 ± 3.65	277.61 ± 2.47	0.41 ± 0.31
DN3	272.47 ± 5.12	262.07 ± 5.32	3.82 ± 0.18
DP1	294.07 ± 6.47	283.02 ± 6.40	3.76 ± 0.61
DP2	291.67 ± 3.07	263.31 ± 3.63	9.72 ± 0.37
DP3	283.07 ± 2.14	272.71 ± 5.19	3.66 ± 0.54
DS1	281.38 ± 1.88	275.64 ± 6.07	2.04 ± 0.22
DS2	278.35 ± 3.12	270.61 ± 3.16	2.78 ± 0.32
DS3	279.30 ± 3.64	269.33 ± 3.14	3.57 ± 0.41
DC1	275.67 ± 3.42	267.28 ± 2.64	3.04 ± 0.25
DC2	284.07 ± 7.23	271.16 ± 3.10	4.54 ± 0.28
DC3	276.81 ± 3.85	265.74 ± 4.21	4.00 ± 0.51

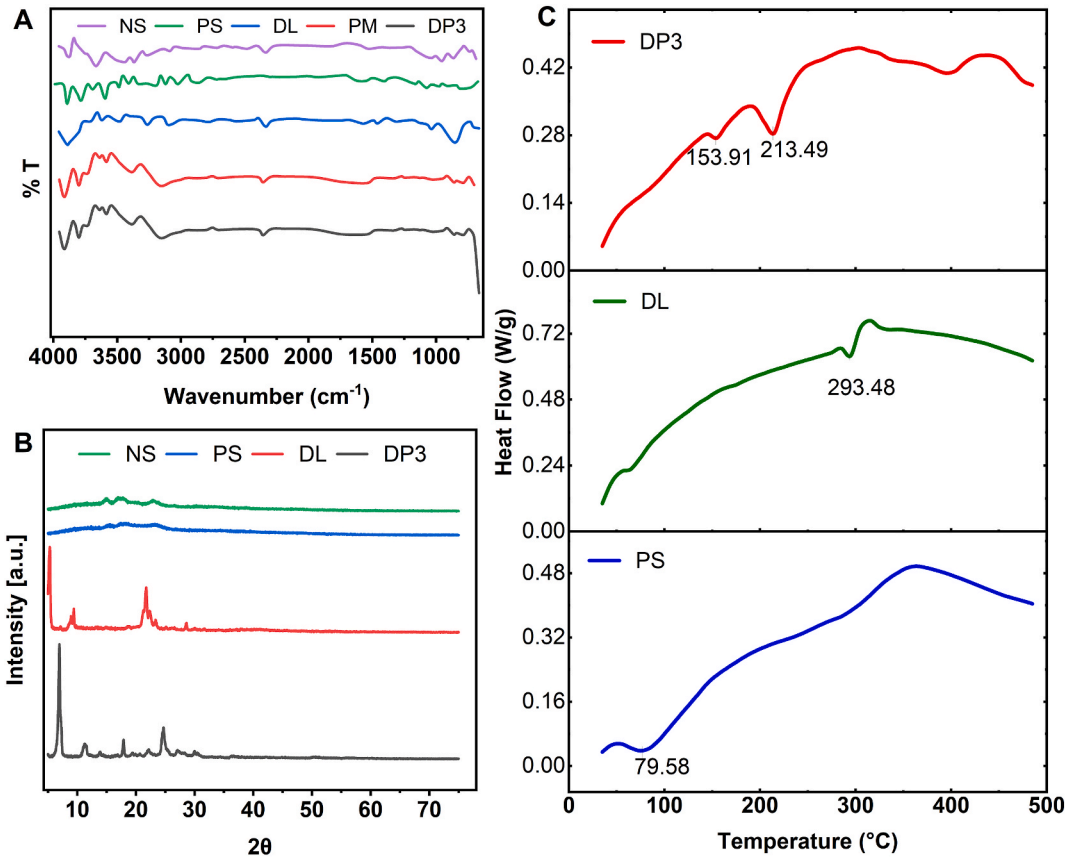

Fig. 3. A) FTIR spectra B) PXRD spectra and C) DSC thermograms. where NS (Neat starch), PS (Porous starch), DL (Diclofenac), PM (Physical mixture), and DP3 (Diclofenac-porous starch Batch 3).

However, the pure DL exhibited sharp diffraction peaks at specific 2θ angles (21.25, 21.76, 23.34, and 28.62°), displaying high intensity and thereby confirming its crystalline nature. Interestingly, in the PXRD spectra of the optimized batch, while some intense peaks were observed, indicating a partial crystalline nature of the drug, there was also evidence of peak shifting compared to the pure DL spectra. This indicates the potential for further optimization of the formulation to maximize these interactions, leading to enhanced dissolution rates and improved tablet performance. From a broader perspective, these findings offer valuable insights into the structural properties of the components involved in the formulation.

3.4.8. Differential scanning calorimetry study (DSC)

In the realm of pharmaceutical formulation, understanding the thermal behavior of key constituents is paramount for designing effective drug delivery systems. The DSC analysis serves as a crucial tool, providing insights into the melting behavior and crystallinity of compounds. Fig. 3C displays the DSC thermogram of *V. radiata* PS, DL, and DP3. DSC thermogram of PS unveiled an endothermic peak at 79.47 °C, indicative of its melting point, while the DL exhibited distinct endothermic peaks at 293.48, 63.47, and 329.13 °C. Notably, the optimized formulation (DP3) displayed a broad endothermic peak at 213.48 °C, suggesting the partial amorphous nature of DL within the formulation. This observed peak shifting is likely attributed to favorable interactions between the drug and excipients. Leveraging these insights, particularly the partial amorphous nature of DL in the optimized formulation, could have informed the design FDTs of DL. Results are in agreement with PXRD results.

3.4.9. Dissolution study

The percentage of cumulative drug release for the formulations DN1-DN3, DP1-DP3, DS1-DS3, and DC1-DC3 ranged from 35.34 % to 60.66 %, 83.96 %–97.65 %, 75.33 %–98.38 %, and 74.30 %–93.00 %, respectively. These results are illustrated in Fig. 4A–D. Notably, the drug release at the 60-min mark for formulations containing NS (DN1-DN3) (Fig. 4A) and croscarmellose sodium (DC1-DC3) (Fig. 4D) was lower compared to PS-based FDTs (DP1-DP3) (Fig. 4B). A significant difference ($p < 0.01$) in drug release at 60 min was observed between NS and PS-based FDTs. The rapid drug dissolution observed in the PS-based FDTs can be attributed to the facile breakdown of particles due to the formation of a porous structure post-sublimation of camphor, facilitating the rapid entry of the drug into the dissolution medium. While PS-based FDTs exhibited similar drug release profiles to batches containing SSG (DS1-DS3) (Fig. 4C) at the 60-min mark, superior results were observed for PS-based FDTs at the initial time points of 10 and 15 min. However, a

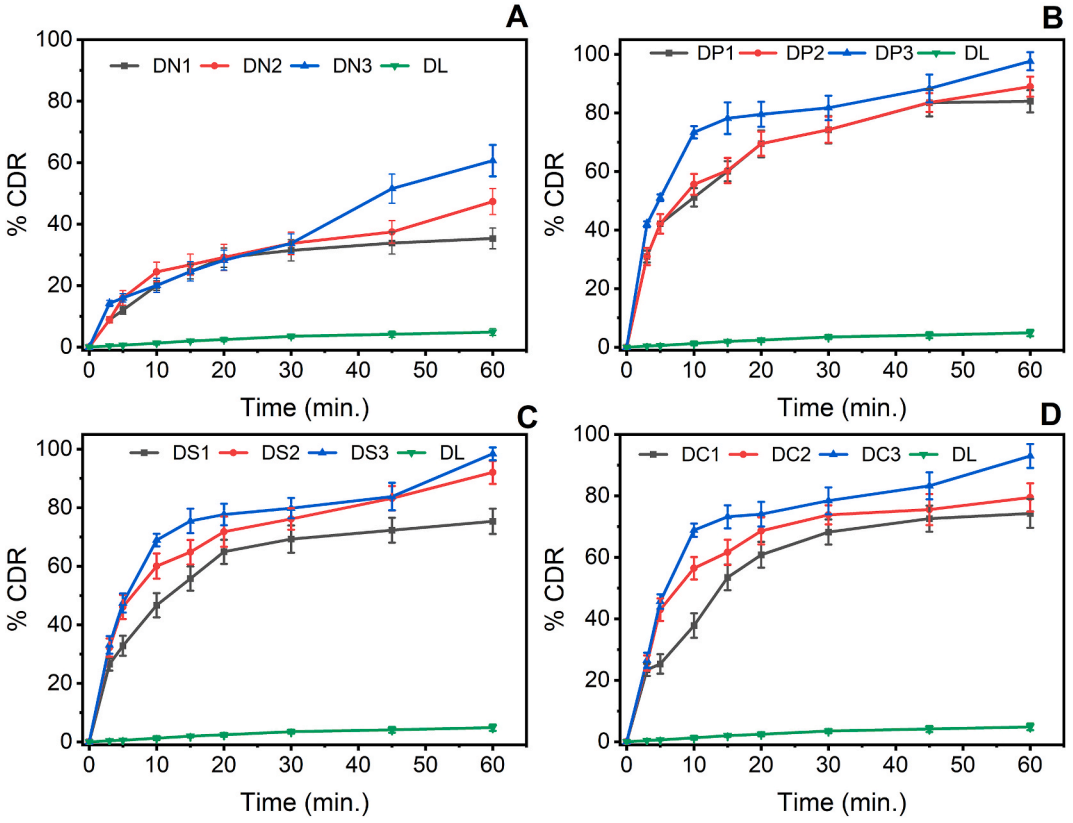

Fig. 4. Plot of % cumulative drug release vs. time for all batches containing A) NS, B) PS, C) SSG and D) CS.

significant difference ($p < 0.05$) in the drug release profile was noted between PS-FDTs and SSG-FDTs at 60 min. Among the PS-containing batches, DP3 demonstrated the highest %DE at each time point (0–60 min). Fig. S3 illustrates model fitting graphs for all batches, with the majority following the Korsmeyer-Peppas model, except for DN2 and DN3, which followed Higuchi-matrix drug release kinetics. Model fitting parameters are shown in Table 6.

As presented in Table 7, the DE10 % for formulations DN1, DN2, and DN3 exhibited remarkable enhancements, showing increases of 28.52, 34.77, and 36.25 folds, respectively, compared to the pure drug DL. Similarly, the DE15 % values for DN1, DN2, and DN3 displayed substantial improvements, with increments of 20.04, 23.74, and 22.49 folds, respectively. Additionally, the dissolution rate was found to be more than 43 folds higher compared to pure DL, indicative of significantly enhanced drug release kinetics. Impressively, DE10 % values for DN1, DN2, and DN3 were elevated by 88.2, 90.95, and 116.75 folds, respectively, relative to pure DL, while DE15 % values exhibited increases of 56.13, 58.10, and 75.2 folds, respectively. Similarly, for formulation DP3, the dissolution rate surpassed that of pure DL by over 174 folds. Moreover, formulations DS1, DS2, and DS3 displayed notable enhancements in DE10 %, with increases of 74.5, 98.05, and 105.3 folds, respectively, compared to pure DL, while DE15 % values showed increments of 49.26, 62.61, and 69.52 folds, respectively. Similarly, formulations DC1, DC2, and DC3 demonstrated substantial improvements in DE10 %, with enhancements of 60.42, 88.92, and 99.55 folds, respectively, compared to pure DL. Correspondingly, DE15 % values for DC1, DC2, and DC3 exhibited increases of 41.77, 57.86, and 66.96 folds, respectively, underscoring the notable enhancements in dissolution efficiency achieved with these formulations.

The observed enhancement in the dissolution rate of crystalline DL can likely be attributed to the incorporation of amorphous excipients such as PS into the formulation. Amorphous excipients have been known to facilitate faster dissolution rates by promoting the rapid disintegration and dissolution of the tablet matrix. In this context, the porous structure of PS, possibly augmented by the sublimation of camphor during tablet preparation, likely provides increased surface area and improved wettability, thus facilitating the rapid release of the drug into the dissolution medium. This enhanced dissolution performance underscores the importance of excipient selection and formulation optimization in achieving desired drug release kinetics and ultimately improving the therapeutic efficacy of the formulated tablets. Porous tablets have demonstrated an enhanced release rate, thereby affirming the potential efficacy of this approach in enhancing the dissolution of loaded drug. This advancement holds promise for optimizing the pharmacokinetic properties and therapeutic efficacy of the medication.

3.4.10. Stability study

Stability investigations spanning a 90-day period were conducted on the prepared porous tablets, with the results meticulously

Table 6
Model fitting data for different batches of DL-FDTs.

Batches	DN1		DN2		DN3		DP1		DP2		DP3	
Model	R	K	R	K	R	K	R	K	R	K	R	K
Zero order	0.5896	0.7993	0.2338	1.9832	0.9193	1.1294	0.1353	1.9402	0.2338	1.9832	0.9132	2.2192
First order	0.7013	−0.0097	0.9053	−0.0413	0.9774	−0.0158	0.8518	−0.0385	0.9053	−0.0413	0.9050	−0.0612
Matrix	0.9596	5.3368	0.9323	13.404	0.9816	7.1566	0.9252	13.1449	0.9323	13.404	0.8296	15.2871
Peppas	0.9692	5.9832	0.9847	23.6856	0.9760	7.1915	0.9837	23.5624	0.9847	23.6856	0.9546	34.7561
Hix. crow.	0.6678	−0.0030	0.7905	−0.0104	0.9654	−0.0047	0.7338	−0.0099	0.7905	−0.0104	0.7276	−0.0135
Batches	**DS1**		**DS2**		**DS3**		**DC1**		**DC2**		**DC3**	
Model	**R**	**K**	**R**	**K**	**R**	**K**	**R**	**K**	**R**	**K**	**R**	**K**
Zero order	0.2261	1.7432	–	2.0436	–	2.1663	0.5716	1.6976	–	1.8587	–	2.0944
First order	0.7581	−0.031	0.9092	−0.0452	0.9108	−0.0610	0.8470	−0.0290	0.6932	−0.0341	0.8619	−0.0478
Matrix	0.9245	11.8157	0.9110	13.8771	0.877	14.7998	0.9579	11.3414	0.8816	12.7211	0.8810	14.3030
Peppas	0.9738	19.2648	0.9737	26.074	0.9420	27.8918	0.9723	14.3802	0.9340	22.4520	0.9142	23.6729
Hix. crow.	0.6509	−0.0082	0.7793	−0.0111	0.8079	−0.0131	0.7813	−0.0080	0.5380	−0.0091	0.7108	−0.0116

Table 7
Comparative Dissolution parameters for the different batches of DL-FDTs and pure DL.

Batches	T50 (min)	DE_{10} %	Increase in DE_{10} (No. of folds)	T90 (min)	DE_{15} %	Increase in DE_{15} %	K_1	Increase in K_1 (No. of folds)
DL	11.41	0.40	–	–	0.75	–	0.1643	–
DN1	16.3	11.41	28.52	56.3	15.03	20.04	5.9832	36.416
DN2	72.7	13.91	34.77	253.0	17.81	23.74	6.5155	39.656
DN3	45.4	14.5	36.25	92.4	16.87	22.49	7.1915	43.77
DP1	4.1	35.28	88.2	35.1	42.10	56.13	19.26	120.37
DP2	7.7	36.38	90.95	45.0	43.58	58.10	26.07	162.93
DP3	6.3	46.70	116.75	36.6	56.40	75.2	27.89	174.31
DS1	4.1	29.80	74.5	35.1	36.95	49.26	19.26	120.37
DS2	7.7	39.22	98.05	45.0	46.96	62.61	26.07	162.93
DS3	6.3	42.12	105.3	36.6	52.14	69.52	27.89	174.31
DC1	16.3	24.17	60.42	56.3	31.33	41.77	13.27	82.93
DC2	10.2	35.57	88.92	48.5	43.40	57.86	20.86	130.37
DC3	7.9	39.82	99.55	35.9	50.22	66.96	22.29	139.31

compared against the initial findings. Following this duration, a marginal increase in hardness and disintegration time was discerned, alongside a negligible rise in friability and a reduction in dissolution rates (at 60 min). However, it is pertinent to note that there were no statistically significant disparities ($p>0.05$) observed in the results obtained from the stability assessments, even after 90-day, when juxtaposed with the initial data. These outcomes robustly affirm the viability of the sublimation technique for crafting porous tablets, highlighting its potential as a robust method for pharmaceutical formulation.

4. Conclusion

This study demonstrates the successful conversion of mung bean NS into PS for the formulation of FDTs prepared using the sublimation method. The integration of PS significantly accelerated the disintegration time of FDTs, offering a notable improvement over NS-FDTs and showing equivalent results compared to conventional superdisintegrant croscarmellose sodium. Analysis of drug-excipient interaction via FTIR revealed no chemical interactions among constituents, ensuring the stability of the formulations. Precompression studies confirmed favorable flow characteristics of the powder blends, supporting the feasibility of the manufacturing process. Compressibility assessments indicated commendable material compressibility, corroborating the suitability of the chosen formulation method. Microscopic examination revealed the formation of pores on the tablet surface, a direct consequence of the sublimation process, contributing to the rapid disintegration of PS-FDTs. Furthermore, dissolution studies demonstrated enhanced drug release rates, particularly notable in PS-FDTs compared to NS, with DP3 exhibiting significant drug release at 60 min. Most batches followed well-established drug release models, ensuring predictability in formulation performance. Stability assessments over 90 days indicated the robustness of PS-based formulations, highlighting their potential for enhancing the dissolution rate of poorly water-soluble drugs. Overall, this research underscores the viability of PS and the sublimation method as promising strategies for the development of efficient fast-dissolving tablets with improved drug release profiles.

Data and code availability statement

Data will be made available on request.

CRediT authorship contribution statement

Sameer J. Nadaf: Writing – review & editing, Visualization, Supervision, Software, Methodology, Conceptualization. **Pranav L. Savekar:** Writing – original draft, Investigation, Data curation. **Durgacharan A. Bhagwat:** Writing – original draft, Resources. **Komal V. Dagade:** Investigation, Data curation. **Shailendra S. Gurav:** Writing – review & editing, Validation, Supervision.

Declaration of competing interest

The authors declare that they have no known competing financial interests or personal relationships that could have appeared to influence the work reported in this paper.

Appendix A. Supplementary data

Supplementary data to this article can be found online at https://doi.org/10.1016/j.heliyon.2024.e38793.

References

[1] M.S. Alqahtani, M. Kazi, M.A. Alsenaidy, M.Z. Ahmad, Advances in oral drug delivery, Front. Pharmacol. 12 (2021), https://doi.org/10.3389/fphar.2021.618411.

[2] V. Parkash, S. Maan, Deepika, S. Yadav, H. Hemlata, V. Jogpal, Fast disintegrating tablets: opportunity in drug delivery system, J Adv Pharm Technol Res 2 (2011) 223–235, https://doi.org/10.4103/2231-4040.90877.

[3] D. Sharma, Formulation development and evaluation of fast disintegrating tablets of salbutamol sulphate for respiratory disorders, ISRN Pharm 2013 (2013) 1–8, https://doi.org/10.1155/2013/674507.

[4] S. Maheshwari, A. Singh, A. Varshney, A. Sharma, Advancing oral drug delivery: the science of fast disintegrating tablets (FDTs), Intelligent Pharmacy (2024), https://doi.org/10.1016/j.ipha.2024.01.011.

[5] D. Sharma, G. Singh, D. Kumar, M. Singh, Formulation development and evaluation of fast disintegrating tablets of salbutamol sulphate, cetirizine hydrochloride in combined pharmaceutical dosage form: a new era in novel drug delivery for pediatrics and geriatrics, J Drug Deliv 2015 (2015) 1–10, https://doi.org/10.1155/2015/640529.

[6] K.S. Remya, P. Beena, P.V. Bijesh, A. Sheeba, Formulation development, evaluation and comparative study of effects of super disintegrants in cefixime oral disintegrating tablets, J. Young Pharm. 2 (2010) 234–239, https://doi.org/10.4103/0975-1483.66794.

[7] V. Suryadevara, S.R. Lankapalli, L.H. Danda, V. Pendyala, V. Katta, Studies on jackfruit seed starch as a novel natural superdisintegrant for the design and evaluation of irbesartan fast disintegrating tablets, Integr Med Res 6 (2017) 280–291, https://doi.org/10.1016/j.imr.2017.04.001.

[8] S. Rambabu, M.S. Ranawat, B. Anil, P. Dinesh, The study of guar gum and starch on disintegration time and drug release of fast dissolving tablet in rabbit using single dose randomized parallel design method, Jordan Journal of Pharmaceutical Sciences 6 (2013) 280–291, https://doi.org/10.12816/0001506.

[9] K. Malik, G. Arora, I. Singh, Locust bean gum as superdisintegrant–formulation and evaluation of nimesulide orodispersible tablets, Polim. Med. 41 (1) (2011) 17–28.

[10] G. Draksiene, D.M. Kopustinskiene, R. Lazauskas, J. Bernatoniene, Psyllium (Plantago ovata forsk) husk powder as a natural superdisintegrant for orodispersible formulations: a study on meloxicam tablets, Molecules 24 (2019), https://doi.org/10.3390/molecules24183255.

[11] B. Vraníková, J. Gajdziok, P. Doležel, The effect of superdisintegrants on the properties and dissolution profiles of liquisolid tablets containing rosuvastatin, Pharmaceut. Dev. Technol. 22 (2017) 138–147, https://doi.org/10.3109/10837450.2015.1089900.

[12] D. Sharma, A. Gupta, J.S. Yadav, Natural superdisintegrant: a key ingredient for orodispersible dosage form, J. Pharm. Negat. Results (8) (2022) 5150–5160, https://doi.org/10.47750/pnr.2022.13.S08.676.

[13] P.K. Dahiya, A.R. Linnemann, M.A.J.S. Van Boekel, N. Khetarpaul, R.B. Grewal, M.J.R. Nout, Mung bean: technological and nutritional potential, Crit. Rev. Food Sci. Nutr. 55 (2015) 670–688, https://doi.org/10.1080/10408398.2012.671202.

[14] D. Hou, L. Yousaf, Y. Xue, J. Hu, J. Wu, X. Hu, N. Feng, Q. Shen, Mung bean (Vigna radiata L.): bioactive polyphenols, polysaccharides, peptides, and health benefits, Nutrients 11 (2019), https://doi.org/10.3390/nu11061238.

[15] M. Zhou, L. Shen, X. Lin, Y. Hong, Y. Feng, Design and pharmaceutical applications of porous particles, RSC Adv. 7 (2017) 39490–39501, https://doi.org/10.1039/c7ra06829h.

[16] S. Sharma, P. Sher, S. Badve, A.P. Pawar, Adsorption of meloxicam on porous calcium silicate: characterization and tablet formulation, AAPS PharmSciTech 6 (4) (2005) E618–E625, https://doi.org/10.1208/pt060476.

[17] S.Y. Singh, L. Kumar, Porous oral drug delivery system: tablets, Pharm. Chem. J. 52 (2018) 553–561, https://doi.org/10.1007/s11094-018-1859-5.

[18] S.Y. Singh, Salwa, R.K. Shirodkar, R. Verma, L. Kumar, Enhancement in dissolution rate of atorvastatin trihydrate calcium by formulating its porous tablet using sublimation technique, J Pharm Innov 15 (2020) 498–520, https://doi.org/10.1007/s12247-019-09397-1.

[19] S.K. Vemula, M. Vangala, Formulation development and characterization of meclizine hydrochloride sublimated fast disintegrating tablets, Int. Sch. Res. Notices 2014 (2014) 1–8, https://doi.org/10.1155/2014/281376.

[20] D. Markl, P. Wang, C. Ridgway, A.P. Karttunen, M. Chakraborty, P. Bawuah, P. Pääkkönen, P. Gane, J. Ketolainen, K.E. Peiponen, J.A. Zeitler, Characterization of the pore structure of functionalized calcium carbonate tablets by terahertz time-domain spectroscopy and X-ray computed microtomography, J Pharm Sci 106 (2017) 1586–1595, https://doi.org/10.1016/j.xphs.2017.02.028.

[21] P.P. Fitwe, R.B. Wakade, J.K. Jadhav, Formulation development and characterization of ondansetron fast dissolving tablet by camphor sublimation, Pharmaceut. Technol. 24 (2000) 52–58, https://doi.org/10.1016/j.jsps.2012.12.005.

[22] K. Neduri, S. Kumar Vemula, V. Kumar Bontha, Different techniques to enhance the dissolution rate of Lovastatin: formulation and evaluation. https://www.researchgate.net/publication/284168350, 2012.

[23] A.L. Estibeiro, D. Harmalkar, S. Godinho, L. Kumar, R.K. Shirodkar, Lacidipine porous tablets: formulation and in vitro characterization, Lat. Am. J. Pharm. 37 (2018) 1764–1771. https://api.semanticscholar.org/CorpusID:105755002.

[24] S.B. Shirsand, S. Suresh, V. Kusumdevi, P.V. Swamy, Formulation design and optimization of fast dissolving clonazepam tablets by sublimation method, Indian J Pharm Sci 73 (5) (2011 Sep) 491–496, https://doi.org/10.4103/0250-474X.98984. PMID: 22923860; PMCID: PMC3425059.

[25] S. Jeevanandham, D. Dhachinamoorthi, K.B.C. Chandra Sekhar, M. Muthukumaran, N. Sriram, J. Joysaruby, Formulation and evaluation of naproxen sodium orodispersible tablets - a sublimation technique, Asian J. Pharm. 4 (2010) 48–51, https://doi.org/10.4103/0973-8398.63985.

[26] A. Abd Elbary, A.A. Ali, H.M. Aboud, Enhanced Dissolution of Meloxicam from Orodispersible Tablets Prepared by Different Methods, vol. 50, Bulletin of Faculty of Pharmacy, Cairo University, 2012, pp. 89–97, https://doi.org/10.1016/j.bfopcu.2012.07.001.

[27] N. Shaheen, S. Uz Zaman, Development of fast disintegrating tablets of flurbiprofen by sublimation method and its in vitro evaluation, Brazilian Journal of Pharmaceutical Sciences 54 (2018), https://doi.org/10.1590/s2175-97902018000417061.

[28] E.S.A. Abdel-Rahman, F.A. El-Fishawy, M.A. El-Geddawy, T. Kurz, M.N. El-Rify, Isolation and physico-chemical characterization of mung bean starches, Int. J. Food Eng. 4 (2008), https://doi.org/10.2202/1556-3758.1184.

[29] R. Punia, M.M. Sharma, D. Kalita, J. Mukhrjee, T. Nayak, H. Singh, Physicochemical, morphological, thermal and pasting characteristics of starches from moth bean (Vigna aconitifolia) cultivars grown in India: an underutilized crop, J. Food Sci. Technol. 54 (2017) 4484–4492, https://doi.org/10.1007/s13197-017-2930-z.

[30] D.N. Dayang, H. Samsudin, U. Utra, A.K. Alias, Modification methods toward the production of porous starch: a review, Crit. Rev. Food Sci. Nutr. (2020) 1–22, https://doi.org/10.1080/10408398.2020.1789064.

[31] M.T. Ali, R. Fule, A. Sav, P. Amin, Porous starch: a novel carrier for solubility enhancement of carbamazepine, AAPS PharmSciTech 14 (2013) 919–926, https://doi.org/10.1208/s12249-013-9985-6.

[32] P.R. Chang, J. Yu, X. Ma, Preparation of porous starch and its use as a structure-directing agent for production of porous zinc oxide, Carbohydr. Polym. 83 (2011) 1016–1019, https://doi.org/10.1016/j.carbpol.2010.08.076.

[33] W.C. Lu, Y.J. Chan, F.Y. Tseng, P.Y. Chiang, P.H. Li, Production and physicochemical properties of starch isolated from djulis (Chenopodium formosanum), Foods 8 (2019), https://doi.org/10.3390/foods8110551.

[34] R. Deveswaran, M. Sravya, S. Bharath, B. V Basavaraj, V. Madhavan, Development of modified porous starch as a carrier to improve aqueous solubility, Adv. Appl. Sci. Res. 3 (1) (2012) 162–170.

[35] Patricia Martínez, Fiorela Peña, Luis A. Bello-Pérez, Carmen Núñez-Santiago, Hernani Yee-Madeira, Carmen Velezmoro, Physicochemical, functional and morphological characterization of starches isolated from three native potatoes of the Andean region, Food Chem. X 2 (2019) 100030, https://doi.org/10.1016/j.fochx.2019.100030.

[36] A.R. Ariyantoro, A. Yulviatun, D.R. Affandi, A. Septiarani, The effect of moisture content and time of heat moisture treatment (HMT) on the properties of jack bean (Canavalia ensiformis) starch, in: IOP Conf Ser Earth Environ Sci, Institute of Physics, 2022, https://doi.org/10.1088/1755-1315/1018/1/012028.

[37] S. Killedar, H. more, S. Nadaf, A. Nale, A. Pawar, U. Tamboli, Isolation, characterization, and evaluation of Cassia fistula Linn. seed and pulp polymer for pharmaceutical application, Int J Pharm Investig 4 (2014) 215, https://doi.org/10.4103/2230-973x.143128.

[38] P. Jaiswal, K.J. Kumar, Physicochemical properties and release characteristics of starches from seeds of Indian Shahi Litchi, Int. J. Biol. Macromol. 79 (2015) 256–261, https://doi.org/10.1016/j.ijbiomac.2015.04.050.
[39] A. Okunlola, O.A. Odeku, Compressional characteristics and tableting properties of starches obtained from four Dioscorea species, FARMACIA 57 (6) (2009) 756–770.
[40] P. Juneja, B. Kaur, O.A. Odeku, I. Singh, Development of corn starch-neusilin UFL2 conjugate as tablet superdisintegrant: formulation and evaluation of fast disintegrating tablets, J Drug Deliv 2014 (2014) 1–13, https://doi.org/10.1155/2014/827035.
[41] V. Dave, R.B. Yadav, R. Ahuja, S. Yadav, Formulation Design and Optimization of Novel Fast Dissolving Tablet of Chlorpheniramine Maleate by Using Lyophilization Techniques, vol. 55, Bulletin of Faculty of Pharmacy, Cairo University, 2017, pp. 31–39, https://doi.org/10.1016/j.bfopcu.2016.12.001.
[42] S. Nadaf, P. Nnamani, N. Jadhav, Evaluation of prosopis africana seed gum as an extended release polymer for tablet formulation, AAPS PharmSciTech 16 (2015) 716–729, https://doi.org/10.1208/s12249-014-0256-y.
[43] N.R. Kotagale, C.J. Patel, A.P. Parkhe, H.M. Khandelwal, J.B. Taksande, M.J. Umekar, Carbopol 934-sodium alginate-gelatin mucoadhesive ondansetron tablets for buccal delivery: effect of pH modifiers, Indian J Pharm Sci 72 (4) (2010 Jul) 471–479, https://doi.org/10.4103/0250-474X.73912.
[44] S. Eraga, M. Ikhuoria Arhewoh, M. Iwuagwu, P.J. Pharm Sci, S. Okhuelegbe Eraga, J. Olamiposi Agboola, M. Amara Iwuagwu, Preliminary investigations of banana (Musa paradisiaca) starch mucilage as binder in metformin tablet formulation. https://www.researchgate.net/publication/328693849, 2018.
[45] K. Anjali, S.P. Manjul, A new approach to enhance the solubility of famotidine tablet by using naturally isolated pear starch, Recent Pat. Drug Deliv. Formulation 12 (2018) 75–80, https://doi.org/10.2174/1872211312666180105113037.
[46] I.B. Pathan, P.R. Shingare, P. Kurumkar, Formulation design and optimization of novel mouth dissolving tablets for venlafaxine hydrochloride using sublimation technique, J. Pharm. Res. 6 (2013) 593–598, https://doi.org/10.1016/j.jopr.2013.04.054.
[47] E. Hellberg, A. Westberg, P. Appelblad, S. Mattsson, Evaluation of dissolution techniques for orally disintegrating mini-tablets, J. Drug Deliv. Sci. Technol. 61 (2021), https://doi.org/10.1016/j.jddst.2020.102191.
[48] S. Abd El Rasoul, G.A. Shazly, Propafenone HCl fast dissolving tablets containing subliming agent prepared by direct compression method, Saudi Pharmaceut. J. 25 (2017) 1086–1092, https://doi.org/10.1016/j.jsps.2017.05.003.
[49] B. Basu, A. Bagadiya, S. Makwana, V. Vipul, D. Batt, A. Dharamsi, Formulation and evaluation of fast dissolving tablets of cinnarizine using superdisintegrant blends and subliming material, J Adv Pharm Technol Res 2 (2011) 266–273, https://doi.org/10.4103/2231-4040.90885.
[50] S.B. Shirsand, S. Suresh, V. Kusumdevi, P. V Swamy, Formulation Design and Optimization of Fast Dissolving Clonazepam Tablets by Sublimation Method, n.d. www.ijpsonline.com.
[51] N.G. Raghavendra Rao, M. Kumar, M.S. Reddy, C. Kistayya, B.M. Reddy, Development and evaluation of fast dissolving tablets of fosinopril by sublimation method. www.ijpsdr.com, 2012.
[52] R. Hoover, Y.X. Li, G. Hynes, N. Senanayake, Physicochemical characterization of mung bean starch, Food Hydrocoll 11 (1997) 401–408, https://doi.org/10.1016/S0268-005X(97)80037-9.
[53] S. Nadaf, A. Jadhav, S. Killedar, Mung bean (Vigna radiata) porous starch for solubility and dissolution enhancement of poorly soluble drug by solid dispersion, Int. J. Biol. Macromol. 167 (2021) 345–357, https://doi.org/10.1016/j.ijbiomac.2020.11.172.
[54] A.S. Ajala, A.O. Aboiye, J.O. Popoola, J.A. Adeyanju, Drying characteristics and mathematical modelling of cassava chips, Chem. Process Eng. Res. 4 (2012) 1–9.
[55] O.D. Akin-Ajani, O.A. Itiola, O.A. Odeku, Effect of acid modification on the material and compaction properties of fonio and sweet potato starches, Starch/Staerke 66 (2014) 749–759, https://doi.org/10.1002/star.201300280.
[56] S. Abd El Rasoul, G.A. Shazly, Propafenone HCl fast disintegrating tablets containing subliming agent prepared by direct compression method, Saudi Pharmaceut. J. 25 (2017) 1086–1092, https://doi.org/10.1016/j.jsps.2017.05.003.
[57] L. Zhang, L. Zhong, P. Wang, L. Zhan, Y. Yangzong, T. He, Y. Liu, D. Mao, X. Ye, Z. Cui, Y. Huang, Z. Li, Structural and functional properties of porous corn starch obtained by treating raw starch with AmyM, Foods 12 (2023), https://doi.org/10.3390/foods12173157.
[58] O.A. Odeku, B.L. Akinwande, Effect of the mode of incorporation on the disintegrant properties of acid modified water and white yam starches, Saudi Pharmaceut. J. 20 (2012) 171–175, https://doi.org/10.1016/j.jsps.2011.09.001.
[59] B. Basu, A. Bagadiya, S. Makwana, V. Vipul, D. Batt, A. Dharamsi, Formulation and evaluation of fast disintegrating tablets of cinnarizine using superdisintegrant blends and subliming material, J Adv Pharm Technol Res 2 (2011) 266–273, https://doi.org/10.4103/2231-4040.90885.
[60] A.Y. Zheng, P.W.S. Heng, L.W. Chan, Tablet disintegratability: sensitivity of superdisintegrants to temperature and compaction pressure, Pharmaceutics 14 (2022), https://doi.org/10.3390/pharmaceutics14122725.
[61] S.L. Shid, S.P. Hiremath, S.N. Borkar, V.A. Sawant, V.S. Shende, M. V Tote, R.B. Birari, S.R. Changrani, Effect of superdisintegrants in rapidly disintegrating flurbiprofen sodium orodispersible tablets via direct compression and camphor sublimation, Journal of Global Pharma Technology 2 (2010) 107–117.